TECHNIQUES FOR THE MEASUREMENT OF ELECTRICAL PROPERTIES OF CORES IN THE FREQUENCY RANGE 10 Hz TO 10 MHz

Ali A. Garrouch and Mukul M. Sharma
The University of Texas at Austin

ABSTRACT

Two and four-electrode techniques have been used to measure the complex impedance of 14 tight gas sand samples, Berea sandstone, and Ottawa sand-bentonite packs in the frequency range of 10 Hz to 10 MHz.

A four-electrode circuit is designed for complex impedance measurement of rocks as well as of sand packs from 10 Hz to 1 MHz. It operates in conjunction with a high pressure resistivity cell that allows measurements while fluid is flowing through the sample. This four-electrode setup offers a number of advantages over the simple two-electrode setup. The latter requires measurements on the sample at two or more different sample thicknesses to be able to quantify the contact impedance at the sample/electrode interface. This is a tedious and time consuming process. The four-electrode setup, however, eliminates the contact impedances at the current electrodes in addition to providing measurements at overburden stress. Perhaps the biggest advantage is the ability to make measurements on partially saturated samples desaturated uniformly by a displacement process. For situations where two-electrode measurements needed to be made, electric field fringing at the disc edges and contact impedances have been quantified and eliminated from the measured signals.

INTRODUCTION

Brine saturated rocks have been reported to display high values (up to 10^5) of dielectric constant at low frequencies (Sen, 1981). This high dielectric response has been attributed to double layer polarization for frequencies less than 10 MHz. Hence, complex impedance measurements become a potentially useful tool in characterizing the clay content and fluid saturations in a rock. Before such interpretations can be made accurate lab measurements of dielectric constant need to be made on partially saturated core samples. Dielectric measurement of partially saturated rocks is, however, an intricate task that needs some improvement in the methodology of the measurement itself. Most of the data for dielectric constant measurements of rocks that is available to date in the literature has been performed with the two-electrode technique (Scott et al., 1967; Knight et al., 1985; and Ruffet et al., 1991). When using this technique, the complex impedance of rocks is typically measured with the help of an impedance analyzer by placing a thin cylindrical disc of the rock between two current electrodes. By assuming that the rock behaves as a parallel resistor-capacitor, its dielectric constant is computed as follows :

$$k = \frac{t_a c_p}{A\varepsilon_o} \qquad (1)$$

k : dielectric constant
t_a : sample thickness (m)
c_p : measured capacitance of disk assuming parallel capacitor model (Farad)

A : cross sectional area of rock sample (m^2)

ε_o : permittivity of air (8.854E-12 $coul^2/Nm^2$)

Scott et al. minimized the electrode polarization and the contact stray impedances, using this measurement technique. They made dielectric constant and conductivity measurements on more than 67 partially saturated rock samples with a two-electrode setup from 100 Hz to 1 MHz. The electrodes used in the Scott et al. study were made of platinized platinum plates and blotter pads. The blotter pads were discs cut from blotter paper and saturated with a weak electrolyte suspension of silver and silver chloride. These pads were placed against the ends of cylindrical rocks that were 1" in diameter and were either 1" or 0.5" long. Platinized platinum plates when used with the blotter pads reduced the electrode polarization errors. Indeed, the large effective area of the platinized surface reduces the series resistance at the metal/solution interface so that its effect on the rock permittivity may become small. The blotter pads saturated with a weak silver and silver chloride suspension minimize the ion build-up at the electrodes since silver ions in solution can enter the pad, discharge and become atoms of metallic silver; or silver atoms can leave the other pad and enter the silver chloride solution in the rock sample as a charged silver ion. Since the chemical reaction between the electrolyte solution in the rock sample and the blotter pads is nearly reversible, this electrode-electrolyte combination can be regarded as reversible.

In summary, even though the two-electrode method of measurement is simple in principle, it has many serious shortcomings. The following list illustrates many of the handicaps of the two-electrode measurement technique used in the past :

1. It is vulnerable to electrode impedances generated at the rock sample/electrode interface. Electrode contact impedances are inevitable because of rock rough surfaces . Even platinum sputtering of the electrodes is not guaranteed to help in this regard because of the scratching that can happen with repeated measurement at the rock/electrode interface. Platinum sputtering might help only if it is repeated frequently.
2. If the sample is poorly protected from air, results will be affected by evaporation. This causes the dielectric response of the rock to drift while the measurement is being made. The dielectric response will not represent the behavior of the rock at the assumed saturation, as a consequence.
3. This measurement is time consuming for low permeability rocks, since it takes a long time (up to 20 days) for the disc sample salinity to come to equilibrium at a desired salinity.
4. Inherent in this measurement is the assumption that the rock behaves like a parallel capacitor which may or may not be true. Thus, in essence an "effective dielectric constant" for the rock is computed.
5. Most of the two-electrode data available is uncorrected for contact impedances.

A very small volume of four-electrode data is available in the literature, namely that of Lockner and Byerlee (1985) who measured the complex impedance of compacted rocks from 10^{-3} Hz to 100 Hz, Myers and Saville (1989) who measured the complex impedance of colloidal suspensions at frequencies below 1 KHz and Hoyer and Rumble (1976) who used a four-electrode bridge circuit to measure the complex impedance of sandstone cores and clay water suspensions from 10 Hz to 0.1 MHz.

The aim of this paper is to present some refinements of the two-electrode technique in the frequency range of 10 Hz to 10 MHz. This paper also describes a high frequency (10 Hz to 1 MHz) four-electrode setup that allows for complex rock impedance measurements under radial stress values of up to 5000 psi while fluids are flowing through the rock samples at a specified pore pressure.

EXPERIMENTAL SETUP AND PROCEDURE

Two-Electrode Measurements

The first set of experiments consisted of measuring the complex impedances of 14 tight gas sand cores saturated with NaCl brine solution at frequencies ranging from 10 Hz to 10 MHz. The cores, whose minerological data is summarized in Table 1., have thicknesses ranging from 3 to 10 mm and are 1.5" in diameter. These measurements are made using an HP 16451B dielectric fixture in conjunction with an HP LCR meter 4192A LF. This test fixture has the advantage of eliminating electric field fringing effects at the edges of the disc material placed between two measuring electrodes . A built-in guard electrode surrounds the measuring electrode to align the electric field at the edges of the disc so that it is perpendicular to the sample face. Consequently, stray capacitances due to edge effects are eliminated. To prevent evaporation, the edges of the tight gas sand discs were coated with a thin film of lucite-chloroform glue and wrapped with a water resistant plastic tape . To completely saturate the discs, they were first saturated with CO_2 at 2000 psi. The samples were then reevacuated and NaCl brine solution (20K ppm) was used to vacuum saturate these discs. Since these cores have low permeabilities, they were pressurized to 2000 psi to ensure that the brine enters all the micropores. Any residual CO_2 will dissolve in the saturating brine. The samples were weighed before and after the impedance measurements to ensure that evaporation effects were insignificant.

Series mode impedances were measured on pairs of discs of different thicknesses. Readings between 10 MHz and 10 Hz stabilized in about one minute. Both the contact resistance and reactance were corrected for as follows :

$$Z_{m1} \cos \theta_1 = R_{t1} + R_c \qquad (2)$$

$$Z_{m2} \cos \theta_2 = R_{t2} + R_c \qquad (3)$$

$$R_{t1} = t_1 R' \qquad (4)$$

$$R_{t2} = t_2 R' \qquad (5)$$

Z_{m1} and Z_{m2} are the measured impedance values for discs 1 and 2, respectively.
θ_1 and θ_2 are the measured phase angles for discs 1 and 2, respectively.
R_{t1} and R_{t2} are the corrected resistances for discs 1 and 2, respectively.
R' is the true resistance per unit thickness for the rock sample.
t_1 and t_2 are the thicknesses of discs 1 and 2 , respectively.
R_c is the contact resistance, assumed the same for discs 1 and 2.

A simple manipulation of equations (2) through (5) gives expressions for the true resistances of discs 1 and 2 :

$$R_{t1} = (z_{m2} \cos\theta_2 - z_{m1}\cos\theta_1)\left(\frac{t_1}{t_2 - t_1}\right) \qquad (6)$$

$$R_{t2} = (z_{m2} \cos\theta_2 - z_{m1}\cos\theta_1)\left(\frac{t_2}{t_2 - t_1}\right) \qquad (7)$$

A similar analysis on the out of phase component of the measured impedances gives the following expressions for the true reactances of discs 1 and 2 :

$$X_{t1} = (z_{m2}\sin\theta_2 - z_{m1}\sin\theta_1)\left(\frac{t_1}{t_2 - t_1}\right) \qquad (8)$$

$$X_{t2} = (z_{m2}\sin\theta_2 - z_{m1}\sin\theta_1)\left(\frac{t_2}{t_2 - t_1}\right) \qquad (9)$$

where X_{t1} and X_{t2} are the true reactances of discs 1 and 2, repectively.

This method of contact resistance and reactance correction inherently assumes that, going from the first disc of thickness t_1 to the second disc of thickness t_2, the contact impedance remains constant. In general, the contact resistances and reactances were small compared to the magnitude of the measured impedances above 1 KHz (Figure 1). The porosity deduced from the electrical measurements also cross checked the helium porosity measured in the lab prior to the experiment within 2 to 3 porosity units. The following algebra was used to convert the series mode data to equivalent parallel mode data to ultimately compute the dielectric constant :

$$c_p = \frac{c_s}{\omega^2 c_s^2 R_s^2 + 1} \qquad (10)$$

c_p : calculated capacitance of disk assuming parallel capacitor model (Farad)
c_s : measured series mode capacitance (Farad)
R_s : measured series mode resistance (Ohm)
ω : angular frequency (Radian*Hz).

The two-electrode setup was calibrated with a polyvinyl chloride sample disc that displayed a constant dielectric constant of 1.8 from 10 KHz to 10 MHz. This result is consistent with tabulated data for polyvinyl chloride. As shown in Figure 2 the two-electrode data of this study compares reasonably well with the data presented by Wong (1983) . The two-electrode data , as displayed in Figure 3, showed some scatter when compared to the estimated data based on Scott et al. empirical model that relates the dielectric constant to the frequency as follows :

$$k = 58{,}140\ \sigma_{100}^{0.5151} f^{-0.597} \qquad (11)$$

where k is the dielectric constant, σ_{100} is the conductivity at 100 Hz (in millimhos/m) and f is the frequency in Hz. The data presented by Scott et al. displayed a similar scatter around this empirical model estimate.

Four-Electrode Measurements

The four-electrode measurement technique, in general, has the advantage of eliminating contact impedances. A schematic of the four-electrode setup is shown in Figures 4a and 4b and the method is illustrated as follows :
Let

Z_m: be the internal impedance of the voltmeter

V_3: the actual potential at point 3
V_4: the actual potential at point 4
Z_{c3}: the measuring voltage probe contact impedance at point 3
Z_{c4}: the measuring voltage probe contact impedance at point 4
Z_x: the core impedance between the two voltage measuring electrodes
I_m : the current drawn by the voltmeter.

Then it follows that :

$$V_3 - V_4 = I_m (Z_{c3} + Z_{c4} + Z_m) \quad (12)$$

$$V_{meter} = I_m Z_m \quad (13)$$

If $Z_m >> (Z_{c3} + Z_{c4})$, then it follows from equations (12) and (13) that :

$$V_3 - V_4 = V_{meter} \quad (14)$$

The above result is a direct consequence of the small current drawn by the voltmeter. This result implies that the voltage read by the voltmeter is approximately that of the rock between the two measuring electrodes and is unaffected by the contact impedances at the electrode/rock interface, provided that the voltmeter impedance is sufficiently high to overshadow any possible contact impedances arising from the voltage measuring probes.

A four-electrode circuit, with this configuration, for measuring rock complex impedance from 10 Hz to 1 MHz has been tested . The circuit connects to a Hassler type core holder that allows electric measurements on rock samples and sand packs at a chosen combination of radial and axial stresses varying from ambient pressure to 5000 psi. The rock sample holder has two current electrodes, connecting to the ends of the core, and two ring voltage measuring electrodes built into the rubber sleeve that holds the rock sample. The four-electrode setup is illustrated in Figure 5 and consists of the following :
1. Two custom operational amplifiers to receive and amplify the measured signals.
2. HP4192A LF (LCR meter) used for differential gain-phase mode measurement.
3. An oscilloscope to cross check gain and phase values read by the LCR meter, and to detect any noise interference, or operational amplifier (op-amp) oscillation.

The first circuit (Figure 5) contains two negative-feedback non-inverting op-amps of unit gain, and a differential op-amp with a nominal gain of two. The two single op-amps are chosen to have unit gain for the purpose of maximizing their input impedances (200 megohms). The second circuit contains a single ended op-amp with a nominal gain of three. A low power electrical power supply (±15 volts) was used to feed needed power for the operational amplifiers used in this circuit. Coaxial cables are used to make connections between the instrument, amplifiers, and core holder. Further details about the circuit components are provided in Garrouch (1992).

The circuit is represented in Figure 6. Since the same current is passing throughout, the following formulation applies :

$$V_{ref} = I Z_{ref} \quad (15)$$

If the sum of the contact impedances at the voltage electrodes is insignificant compared to the impedance of the voltmeter, the following approximation can be made :

$$V_{diff} = (V_3 - V_4) = I Z_2 \quad (16)$$

where :

V_3 and V_4 are voltages at the measuring electrodes.
Z_{ref} is the reference impedance (200 ohms).

V_{ref} is the voltage across the reference impedance.
Z_1, Z_2 and Z_3 represent the impedances of the regions of the rock before, between, and after the voltage probes. In Figure 6 the core holder is represented by the solid line and the actual rock sample by the dashed line. Z_{c1} and Z_{c2} represent the contact impedances of the current electrodes. Z_2 is measured by measuring the ratio of V_{diff} to V_{ref}.

$$\frac{V_{diff}}{V_{ref}} = \frac{I Z_2}{I Z_{ref}} = \frac{Z_2}{Z_{ref}} = \frac{Z_2}{200} \tag{17}$$

The LCR meter displays the gain (in Decibels, dB) and the phase in degrees. To obtain the resistance (R) and the reactance (X) from the measured gain and phase, the following algebra is used :

$$|Z_2| = 10^{G/20}\, 200 \tag{18}$$

$$X = |Z_2| \sin\theta \tag{19}$$

$$R = |Z_2| \cos\theta \tag{20}$$

The four-electrode setup was calibrated with RC circuits that have known frequency responses. Independent resistivity measurements with a four-electrode circuit operating at 60 Hz matched data from the new four-electrode setup at 60 Hz within less than 5% for all experimental runs.

As illustrated in Figure 7 the four-electrode data at 0.1 MHz compares within a factor of 2 to 3 with the two-electrode empirical fit of Scott et al.

RESULTS

Two-Electrode Data

After correcting for contact impedances, very reasonable and continuously varying data was obtained using the two-electrode setup down to 10 Hz. Pairs of discs from the same core samples had overlapping resistivity and dielectric constant profiles (Figures 8a and 8b).As shown in Figure 9 the two-electrode data displayed semi-circular impedance plots centered below the resistance axis, indicating a distribution of relaxation times.

We define a lower critical frequency f_c that corresponds to a minimum in the reactance in the impedance plot (Figure 9). This frequency is found to correlate well with a characteristic length, $\sqrt{\frac{K_\infty}{\phi}}$, where K_∞ is the extrapolated liquid permeability and ϕ is the porosity (Figure 10). The characteristic relaxation time τ, which is the inverse of f_c, is found to depend linearly on the square of the characteristic length up to a critical dimension above which τ seemed to be invariant (Figure 11). This dependence between τ and the square of the characteristic length for porous media is analogous to the dependence of the characteristic relaxation time of a single charged sphere upon its radius squared, where τ is defined as the particle radius squared (a^2) divided by the counterion diffusion coefficient (D_1). Even though for a single sphere this dependence of τ upon a^2 stays linear for all values of a^2, for a porous medium this linearity reaches an assymptotic value and is limited by the amount of roughness and tortuosity in the porous medium. This result implies that

the variation of the lower critical frequency from one sample to another could be indicative of the grain size effect on the impedance spectrum. To check the validity of this argument, we used the Lima-Sharma model (Lima and Sharma, 1991 and 1992) to simulate the dielectric response of a charged spherical sand grain subjected to an oscillating field. The dielectric constant of this particle decreased as the particle radius increased (Figure 12). A plot of dielectric constant of the tight gas sand samples versus the characteristic length showed a similar trend (Figures 13a and 13b). Raythatha and Sen (1986) reported a similar trend of decreasing dielectric constant with increasing grain size when they measured the dielectric constant of Na+-hectorite samples of various particle radii in the frequency range 0.5 MHz to 1.3 GHz.

Four-Electrode Data

The four-electrode circuit was used to measure the complex impedance and phase angle of Berea sandstone cores and Ottawa sand-bentonite packs. Oil-wet and water-wet cores and sand-clay packs at different brine/decane saturations, stresses and salinities were used. Sand packs and Berea cores were made oil-wet by saturating them with a solution of 80% isopropyl alcohol and 20% Quilon-C (Sharma et al. , 1991).

The cores and the sand-clay packs were vacuum saturated with NaCl brine solutions of different salinities in the following sequence : 2K ppm, 10K ppm, 20K ppm, then 10K ppm again. This flooding sequence was followed by an n-decane displacement. The reproducibility of the data was checked by going to 100% 10K ppm brine saturation initially from 2K ppm and back from 20K ppm brine, for all experimental runs (Figure 14). Data reproducibility for partial saturations, as well as for independent runs on sand-clay mixtures was checked . All data measured showed a high degree of reproducibility, and were virtually time invariant .

For different salinities, saturations, wettability, stress and clay content the sand and core samples displayed smooth variations in the impedance plots (Figures 15, 16, 17, 18 and 19). These figures clearly imply that the dielectric constant decreases with increasing oil saturation, decreasing salinity, decreasing clay content, increasing stress, and with increasing oil wetness. The resistivity (as shown in the impedance plots) decreases slightly with increasing frequency while the dielectric constant decreases dramatically. This result is consistent with the expected mode of charge transport in porous media. For low frequencies, for instance, charges have sufficient time to travel in the pores before the electric field changes direction. In the course of this travel time, these charges may collide with some pore walls while trying to align themselves with the applied electric field, and hence these collisions increase the bulk resistance to current flow. Whereas for sufficiently high frequencies, these ions travel a shorter distance, before the electric field changes direction, and as a consequence, they collide less frequently with the pore walls. A detailed analysis of this data is presented in Garrouch and Sharma (1992a and 1992b).

CONCLUSIONS

A four-electrode circuit that allows complex impedance measurement of partially saturated rock samples and sand packs at variable stress and fluid saturations in the 10 Hz to 1 MHz range has been tested; and a two-electrode technique for dielectric constant measurements [10 Hz to 10 MHz] is presented. The lower critical frequency of the impedance plot is found to be closely related to the characteristic length of the tight gas sand samples. Consequently, this characteristic frequency can be used as a parameter in the dielectric constant empirical models to incorporate the grain size and tortuosity effects. This result also implies that the impedance spectrum could be used to give an estimate of the permeability.

In the frequency range of 10 Hz to 10 MHz interfacial polarization is the dominant mechanism of charge polarization in porous media. This makes the dielectric constant very

sensitive to the amount of clays present, the brine salinity, the rock geometry (tortuosity and porosity), and to the brine saturation. As a consequence, in this frequency range the dielectric constant can not be used directly from the logs to estimate hydrocarbon and water saturations (as is the case in the gigahertz range). The data presented here has been analyzed in more detail in Garrouch and Sharma (1992a and 1992b).

ACKNOWLEDGMENTS

The authors wish to thank Dr. Francis X. Bostick, Jr. and Dr. Henry F. Dunlap for their valuable suggestions and helpful discussions. The authors also wish to thank Jeff Harrel for his significant contribution in building and testing the four-electrode circuit. Ali Garrouch wants to acknowledge the financial support of the companies sponsoring the Logging and Petrophysics research program.

REFERENCES

Garrouch, A. A., 1992, Dielectric properties of fluid saturated rocks: Ph.D. Dissertation, University of Texas at Austin.

Garrouch, A. A., and Sharma, M. M., 1992a, The influence of clay content, salinity, stress and wettability on the dielectric properties of brine saturated rocks: 10 Hz to 10 MHz: Submitted to Geophysics.

Garrouch, A. A., and Sharma, M. M., 1992b, Dielectric properties of partially saturated rocks: 10 Hz to 10 MHz: Submitted to Geophysics.

Hoyer, W. A., and Rumble, R. C., 1976, Dielectric constant of rocks as a petrophysical parameter, paper O, *in* 17th Annual Logging Symposium Transactions: Society of Professional Well Log Analyst, 28p.

Knight, R. J., Nur, A., and Raistrick, I.D., 1985, Modelling the electrical response of sandstones with an equivalent circuit, paper M, *in* 26th Annual Logging Symposium Transactions: Society of Professional Well Log Analysts, 17p.

Lima, O. A. L., and Sharma, M. M., 1991, Water conductivity and saturation effects on the dielectric response of shaly sands, paper G, *in* 32nd Annual Logging Symposium Transactions: Society of Professional Well Log Analysts, 24p.

Lima, O. A. L., and Sharma, M. M., 1992, A generalized Maxwell-Wagner theory for membrane polarization in shaly sands: *Geophysics*, v. 57, no. 3, p.431-440.

Lockner, D. A., and Byerlee, J. D.,1985, Complex resistivity measurements of confined rock: *Journal of Geophysical Research*, v. 90, no. B9, p. 7837-7847.

Myers, D. F., and Saville D. A. , 1989, Dielectric spectroscopy of colloidal suspensions: *Journal of Colloid and Interface Science*, v. 131, no. 2, p. 448-460.

Raythatha, R., and Sen, P. N., 1986, Dielectric properties of clay suspensions in MHz to GHz range: *Journal of Colloid and Interface Science*, v. 109, no. 2, p. 301-309.

Ruffet, C., Guenguen, Y., and Darot, M., 1991, Complex conductivity measurements and fractal nature of porosity: *Geophysics*, v. 56, no. 6, p.758-768.

Scott, J. H., Carroll, R. D., and Cunningham, D. R., 1967, Dielectric constant and electrical conductivity measurements of moist rock : a new laboratory method: *Journal of Geophysical Research*, v. 72, no. 20, p.5101-5115.

Sen, P. N., 1981, Relation to certain geometrical features to the dielectric anomaly of rocks: *Geophysics*, v. 46, no. 12, p. 1714-1720.

Sharma, M. M., Garrouch, A. A. , and Dunlap, H. F, 1991, Effects of wettability, pore geometry, and stress on electrical conduction in fluid-saturated rocks: *The Log Analyst*, v.32, no. 5, p. 511-526.

Wong, Po-zen, 1983, Fractal surfaces in porous media, *in* American Institute of Physics Conference proceedings, v. 154, p. 304-318.

Table 1. Petrographic data for tight gas sand cores. Both the porosity and the permeability were measured at 800 psi net overburden stress using helium.

Sample	Qu%	K-Fe%	Ka%	Ch%	Il+Sm%	K_∞(md)	Porosity%
100	63	0	4	1	7	0.030	11.9
101	57	0	0	1	18	0.037	13.6
102	62	0	0	1	23	0.028	13.7
108	62	0	0	4	24	0.026	14.1
109	67	2	0	5	15	0.103	13.9
124	66	3	3	3	12	0.013	11.2
126	40	0	2	0	7	0.004	4.4
128	57	3	3	3	15	0.02	10.7
131	66	2	3	2	13	0.062	11.1
133	62	2	6	0	8	0.036	7.0
134	67	0	6	2	8	0.175	8.0
136	61	0	5	0	8	0.005	4.6
140	64	3	11	0	16	0.032	7.7
144	29	0	16	0	42	0.266	7.7

Legend for Table 1:

Qu% : % volume of quartz

K-Fe% : % volume of K-Feldspar

Ka% : % volume of Kaolonite

Ch% : % volume of Chlorite

Il+Sm%: % volume of Illite+Smectite

K_∞ : Permeability

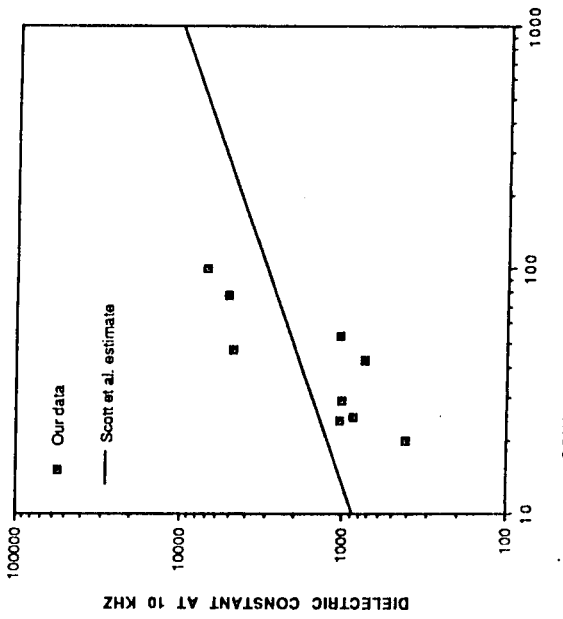

FIG. 3. Comparing our two-electrode data to Scott et al. (1967) empirical model estimate of the dielectric constant at 10 KHz.

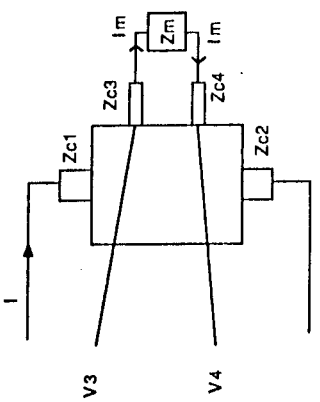

FIG. 4a. Four-electrode setup contact impedance diagram.

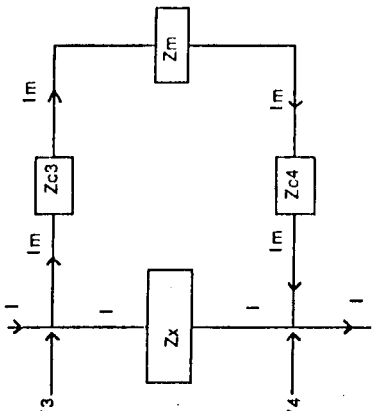

FIG. 4b. Equivalent contact impedance diagram.

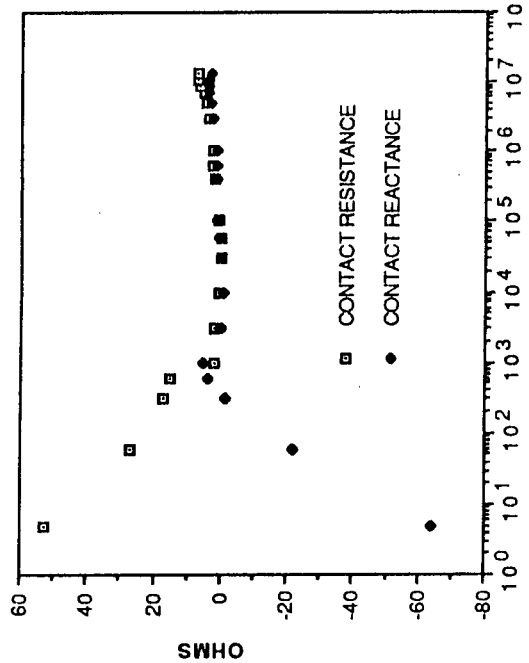

FIG. 1. Contact resistance and reactance for tight gas sand sample# 102 saturated with 20K ppm NaCl brine (two-electrode measurements).

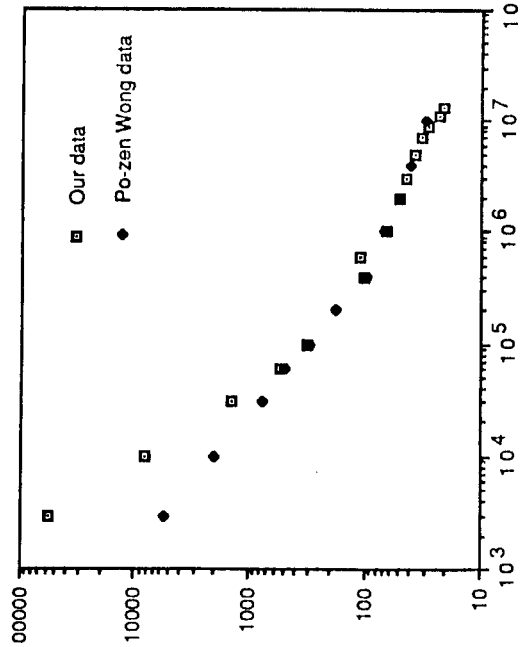

FIG. 2. Dielectric constant for our sample # 144 (58% clays) compared to that of a shaly Portland sandstone from Po-zen Wong (1983) data. Both samples were saturated with 6000 ppm NaCl brine (two-electrode measurements).

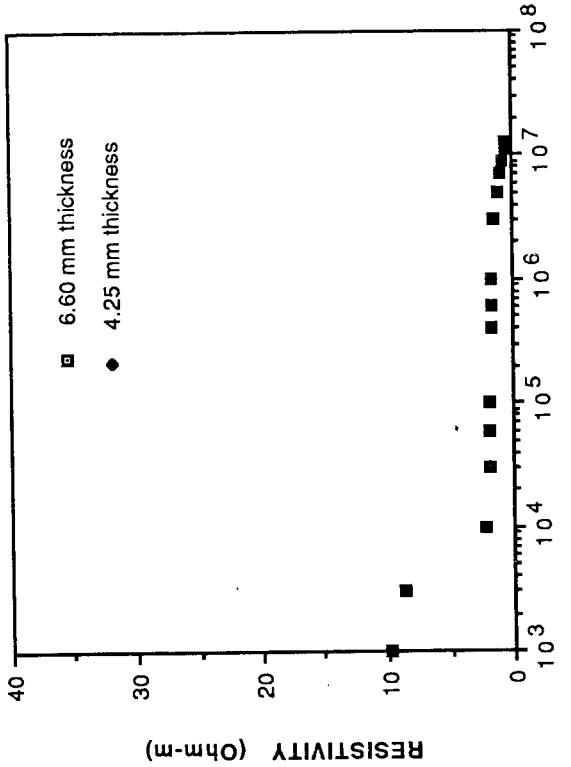

FIG. 8a. Overlapping resistivity for two tight gas sand discs from sample 102 saturated with 20K ppm NaCl brine (two-electrode measurements).

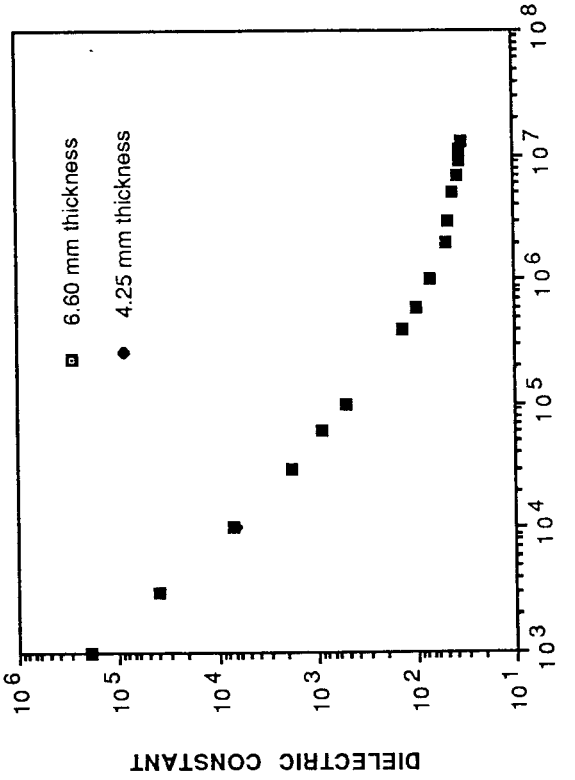

FIG. 8b. Overlapping dielectric constant for two tight gas sand discs from sample # 102 saturated with 20K ppm NaCl brine (two-electrode measurements).

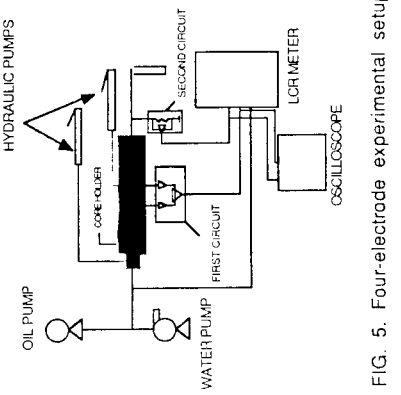

FIG. 5. Four-electrode experimental setup.

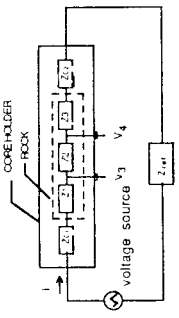

FIG. 6. Schematic diagram of the four-electrode circuit.

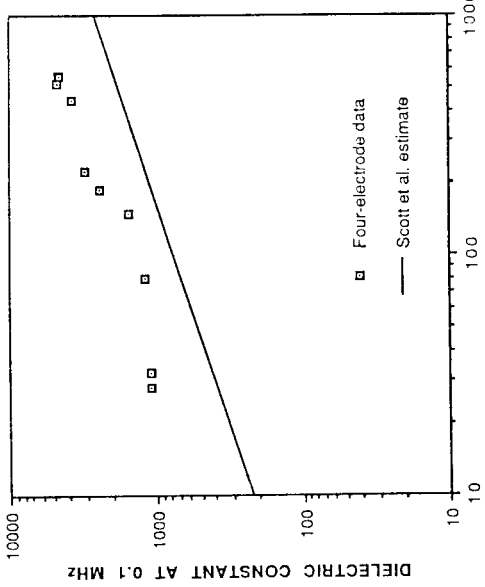

FIG. 7. Comparing our four-electrode data to Scott et al. (1967) empirical model estimate of the dielectric constant at 0.1 MHz.

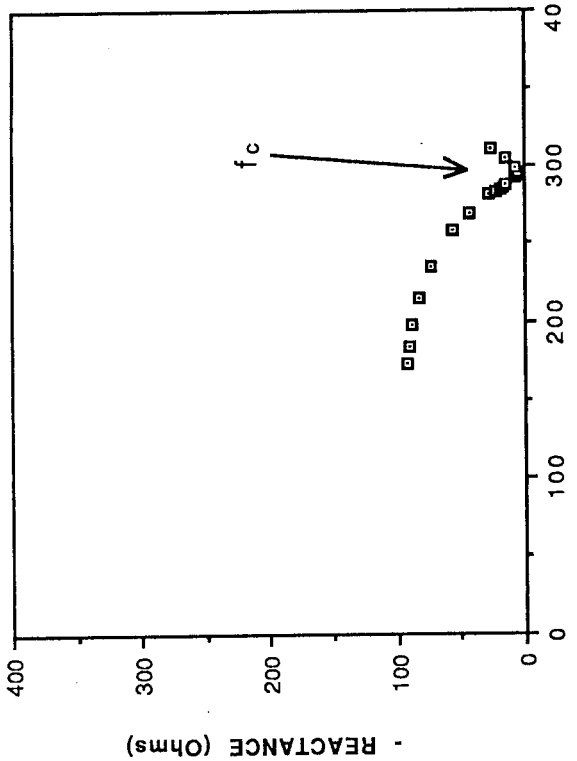

FIG. 9. Impedance plot for sample# 136 (4.95 mm thick) saturated with 20K ppm NaCl brine (two-electrode measurements).

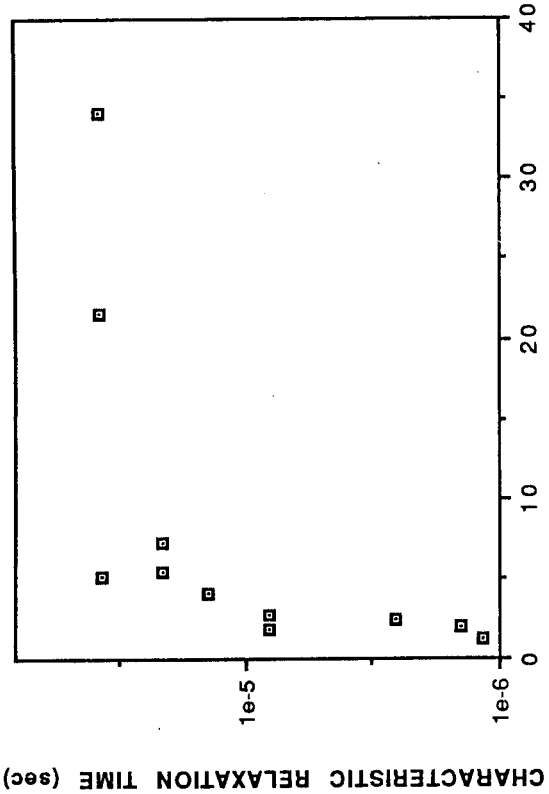

FIG. 11. Characteristic relaxation time versus characteristic length square for tight gas sand samples saturated with 20K ppm NaCl brine (two-electrode measurements).

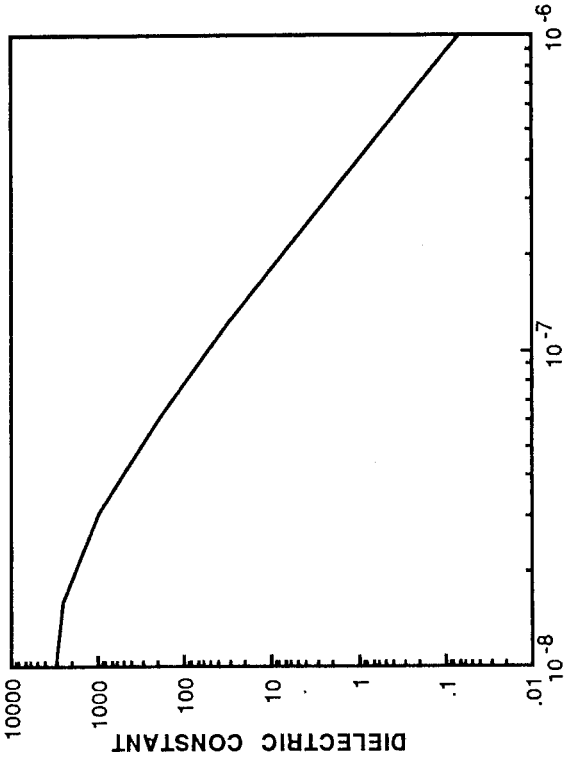

FIG. 12. Calculated dielectric constant for a spherical particle versus particle radius in a 0.1 M NaCl solution using Lima-Sharma model (1991). Surface counterion density is equal to 0.5 E18 ionm/m2.

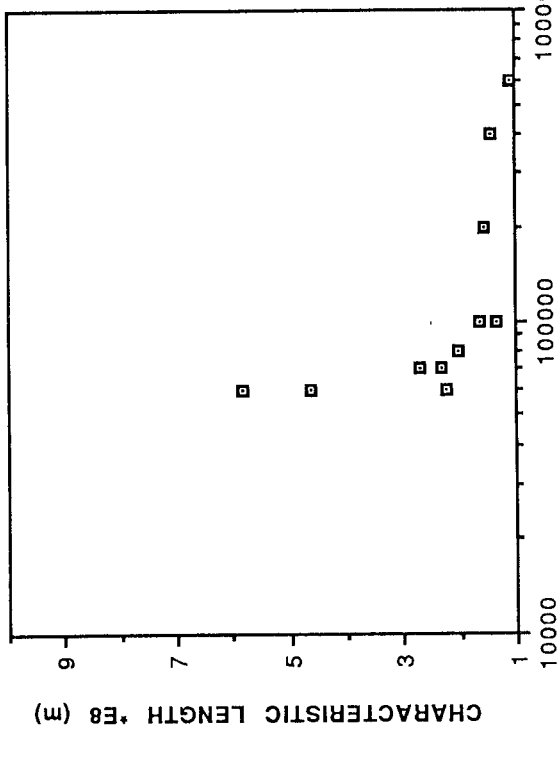

FIG. 10. Characteristic length versus frequency for tight gas sand samples saturated with 20K ppm NaCl brine (two-electrode measurements).

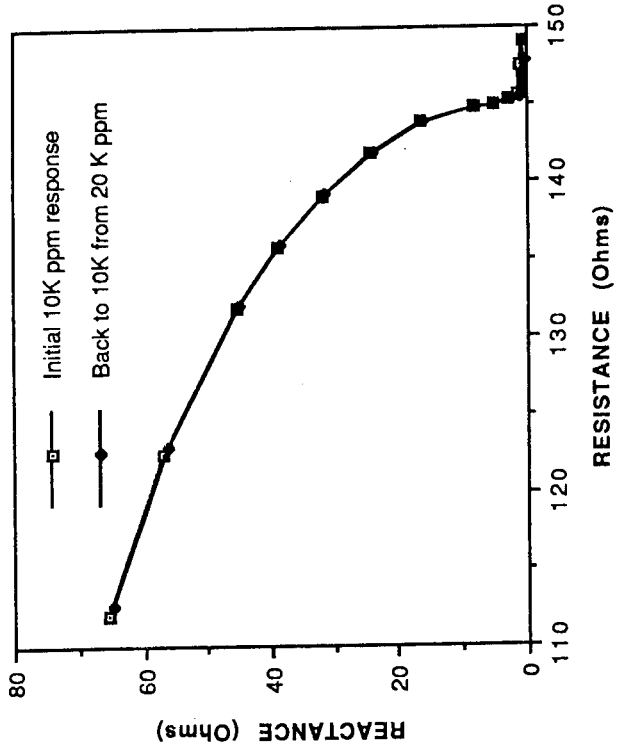

FIG. 14. Impedance plot for two repeat runs on the same water-wet Berea saturated with 10K ppm NaCl brine (four-electrode measurements).

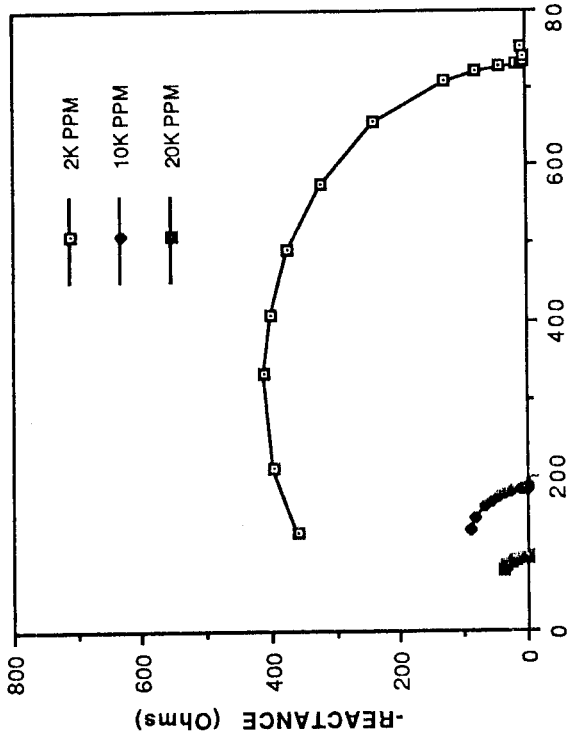

FIG. 15. Impedance plot for oil-wet Berea sandstone saturated with NaCl brine at three different salinities (four-electrode measurements).

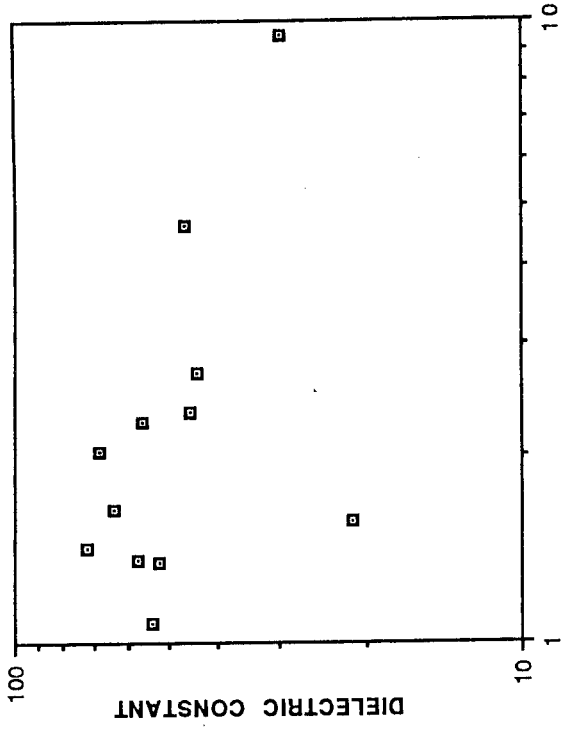

FIG. 13a. Dielectric constant versus characteristic length at 1MHz for tight gas sand samples saturated with 20K ppm NaCl brine (two-electrode measurements).

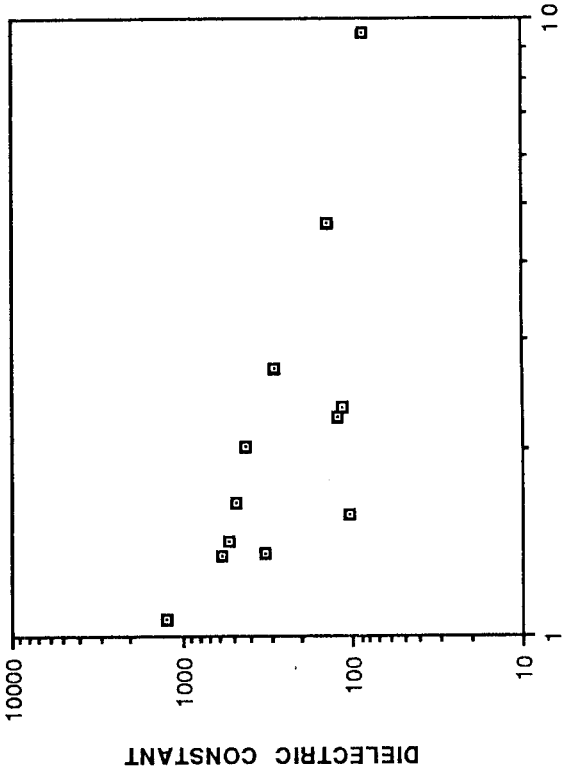

FIG. 13b. Dielectric constant versus characteristic length at .1 MHz for tight gas sand samples saturated with 20K ppm NaCl brine (two-electrode measurements).

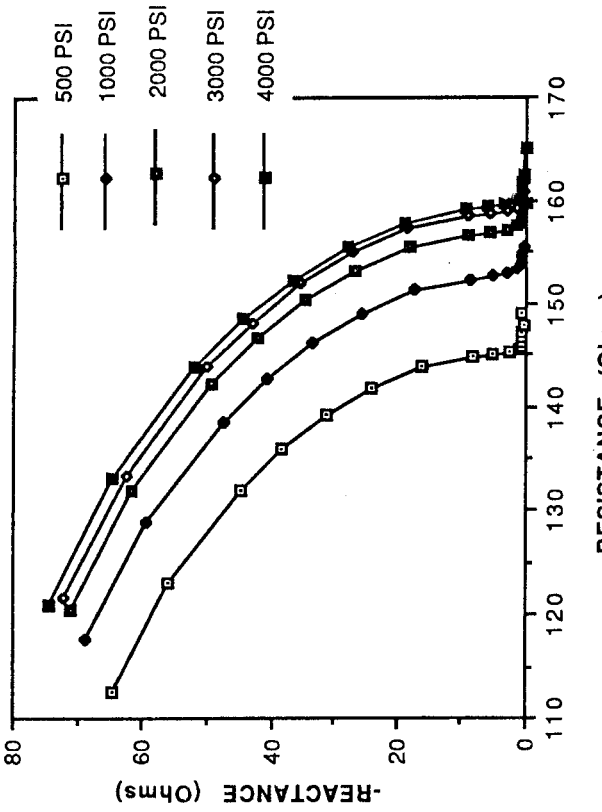

FIG. 18. Impedance plot for water-wet Berea saturated 10K ppm NaCl brine at effective radial stress varying from 500 to 4000 psi. Axial stress = .5 radial stress (four-electrode measurements).

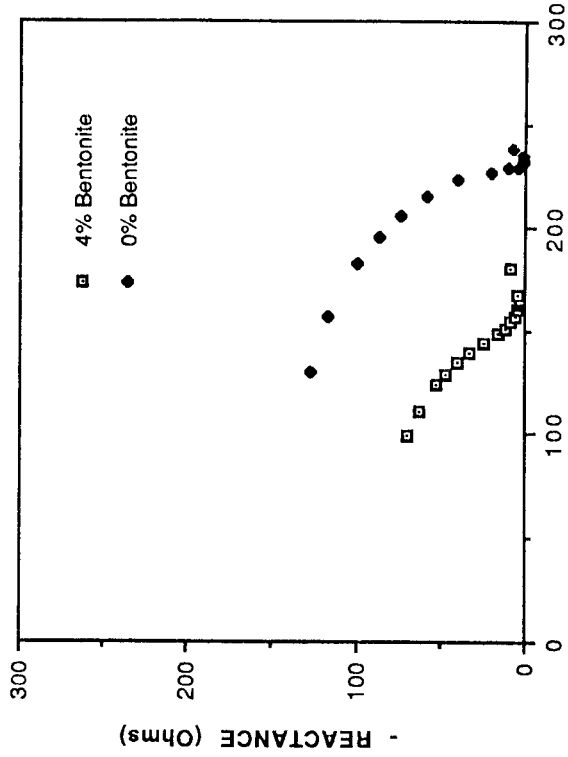

FIG. 19. Impedance plot for two packs of Ottawa sand mixed with 0% and 4% by weight bentonite saturated with 2K ppm NaCl brine (four-electrode measurements).

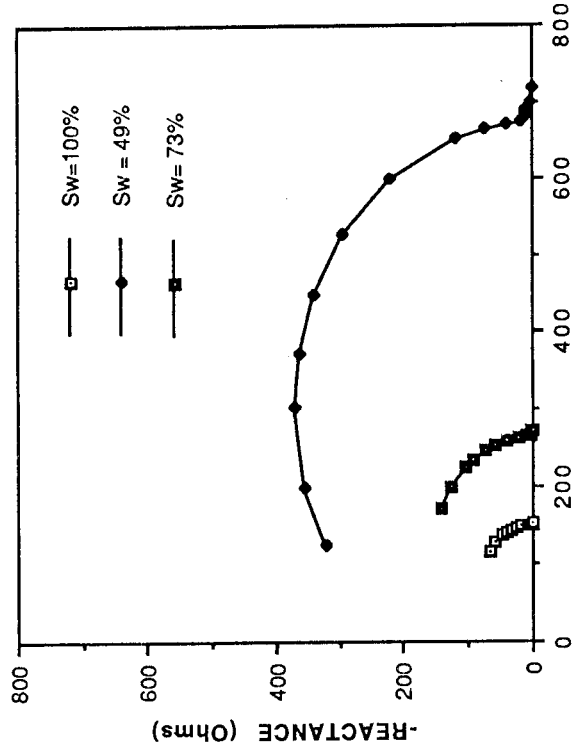

FIG. 16. Impedance plot for water-wet Berea sandstone at three saturations. N-decane and 10K ppm NaCl brine are used (four-electrode measurements).

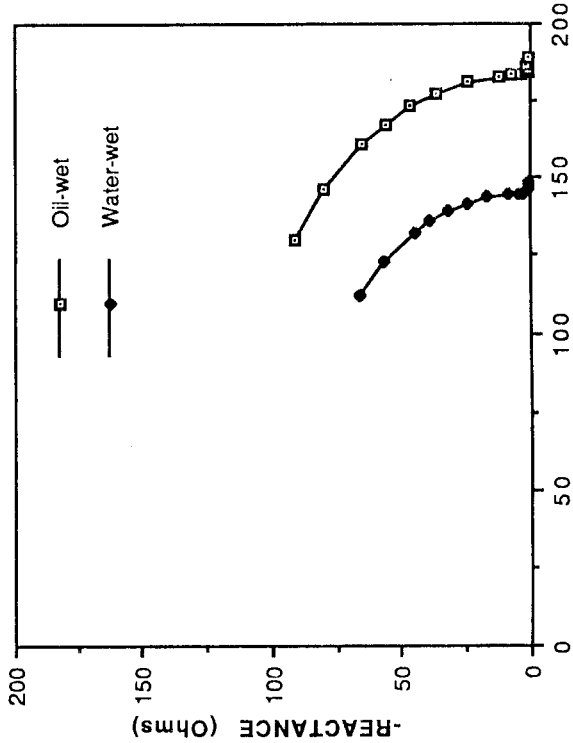

FIG. 17. Impedance plot showing water-wet and oil-wet Berea response saturated with 10K ppm NaCl brine (four-electrode measurements).